





Improving water resistance and mechanical properties of waterborne acrylic resin modified by octafluoropentyl methacrylate

Jialin Bi¹, Zhangyin Yan^{1,8}, Lei Hao², Ashraf Y. Elnaggar³, Salah M. El-Bahy^{4,6}, Fuhao Zhang¹, Islam H. El Azab³, Qian Shao^{1,*} , Gaber A. M. Mersal⁵, Junxiang Wang^{1,*}, Mina Huang^{6,7}, and Zhanhu Guo^{6,7,8,*} 

¹ College of Chemical and Biological Engineering, Shandong University of Science and Technology, Qingdao 266590, China

² Dalian University of Technology, Dalian 116023, China

³ Department of Food Science and Nutrition, College of Science, Taif University, P. O. Box 11099, 21944 Taif, Saudi Arabia

⁴ Department of Chemistry, Turabah University College, Taif University, P.O.Box 11099, 21944 Taif, Saudi Arabia

⁵ Department of Chemistry, College of Science, Taif University, P.O. Box 11099, 21944 Taif, Saudi Arabia

⁶ College of Materials Science and Engineering, Taiyuan University of Science and Technology, Taiyuan 030024, China

⁷ Department of Chemical & Biomolecular Engineering, University of Tennessee, Knoxville, TN 37996, USA

⁸ Integrated Composites Laboratory (ICL), Department of Mechanical and Construction Engineering, Northumbria University, Newcastle Upon Tyne NE1 8ST, UK

Received: 28 April 2022

Accepted: 4 November 2022

Published online:

4 January 2023

© The Author(s), under exclusive licence to Springer Science+Business Media, LLC, part of Springer Nature 2023

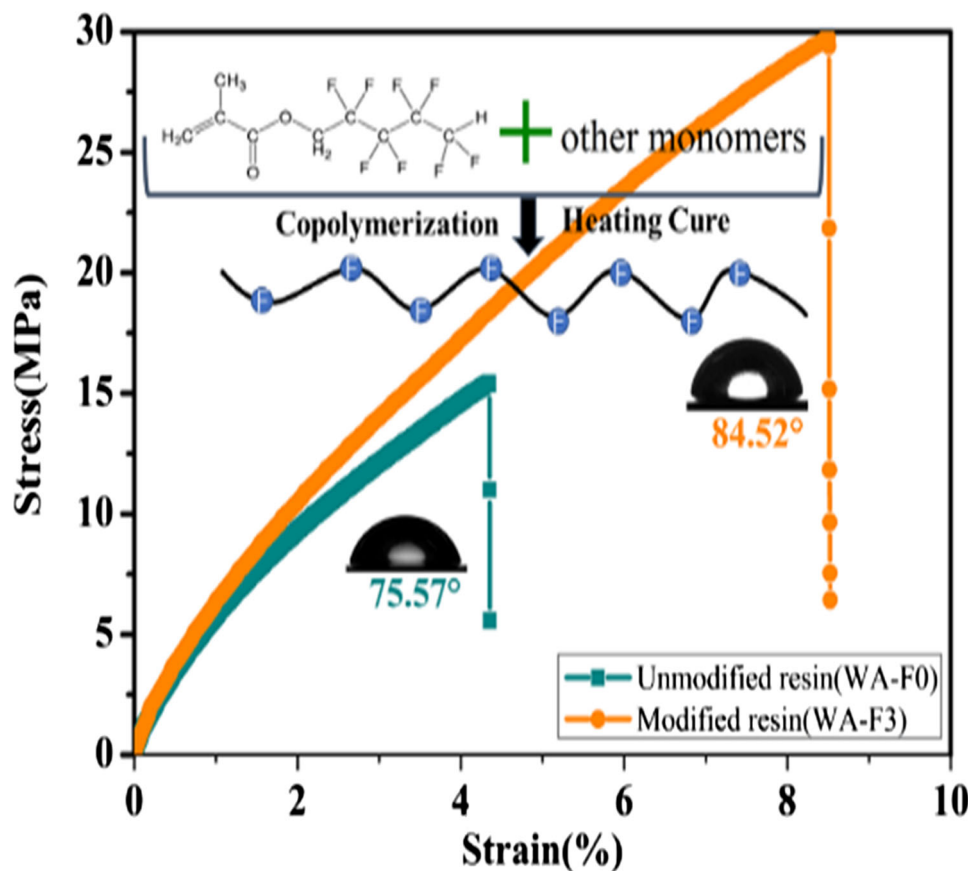
ABSTRACT

A new type of waterborne acrylic resin was prepared by the solution polymerization with octafluoroamyl methacrylate (OF-PMA), 2-butoxy ethanol, and acrylic monomers as raw materials and N, N-dimethyl ethanolamine as pH regulator. Fourier transform infrared spectroscopy and X-ray photoelectron spectroscopy showed that the OF-PMA monomers were successfully grafted onto the resin. The effects of the addition mode and content of OF-PMA on the properties of waterborne acrylic resin were studied. The properties of waterborne acrylic polymer and its coating were tested by a thermogravimetric analyzer, an optical contact angle measuring instrument, and a tensile testing machine. The results showed that after the introduction of OF-PMA monomer into acrylic resin, the tensile strength of the resin was increased by 14.31 MPa. Moreover, the water resistance and heat resistance of resin coating were also improved obviously and the as-modified resin coating exhibited better fullness, adhesion of Gt0, and the hardness of 4H. The novel acrylic resin exhibits a potential application prospect in the fields of waterborne wood coatings.

Handling Editor: Chris Cornelius.

Address correspondence to E-mail: shaoqian@sdust.edu.cn; wangjunxiang1018@sdust.edu.cn; nanomaterials2000@gmail.com

GRAPHICAL ABSTRACT



Introduction

Conventional solvent-based coatings contain high concentrations of volatile organic compounds (VOCs), which can seriously contaminate the atmosphere and cause significant human harm during the production and construction [1–4]. Waterborne resin uses water instead of traditional organic solvents as the main dispersion medium [5, 6]. Its irritation and toxicity are much lower than those of traditional solvent-based resins. It is a green environmental protection product with low VOC. Therefore, the development and utilization of waterborne resin become a research direction with broad development prospects [7–9].

There exists a great variety of waterborne resins, including acrylic resin, epoxy resin [1], polyurethane

[4, 10], fluorocarbon resin [11], and amino resin, among which waterborne acrylic resin is the most-used [12]. Waterborne acrylic resin is primarily polymerized by acrylic acid or methacrylic acid monomer under the action of an initiator, with excellent gloss, and adhesion. However, the disadvantages of poor water resistance and low mechanical strength limit its further applications [13, 14]. To solve these problems, scholars adopt the strategy to modify waterborne acrylic resin with different functional monomers. For example, Bai et al. synthesized hexafluorobutyl methacrylate (HFMA) monomers and prepared a core-shell fluorinated acrylate emulsion. The textile treated with this emulsion demonstrated obvious water repellent and oil repellency [15]. Lei et al. prepared fluorosilicone acrylic resin with HFMA, vinyltrimethoxysilane and 2-[3-

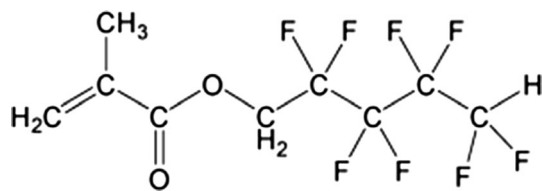


Figure 1 The molecular structure of OF-PMA.

(2H-Benzotriazol-2-yl)-4-hydroxyphenyl ethyl methacrylate as modified monomers, which improved the thermal stability and weather resistance of the resin [16]. Çakmakçi synthesized tripropylene glycol diacrylate fluorinated resin from 2-hydroxyethyl methacrylate, fluoroalcohol and hexamethylene diisocyanate trimer, which enhanced the surface hardness and contact angle of the coating [17]. In the field of resin coatings, fluorine-containing monomers are very important because of the high electronegativity of fluorine atoms [18], which not only changed the surface properties of polymer films but also affected the internal structure of resins [19, 20].

1H,1H,5H-octafluoroamyl methacrylate (OF-PMA), fluorine-containing monomer with double bond at one end, can provide conditions for the co-polymerization of OF-PMA and acrylic monomers, and its specific structure is shown in Fig. 1. Meanwhile, OF-PMA contains a large number of high energy C-F bonds and a large number of low surface energy F atoms. If it can be successfully introduced into the synthesis of acrylic resin, the performance of acrylic resin will be greatly improved.

In this study, in order to improve the water resistance, heat resistance, and mechanical properties of waterborne acrylic resin, OF-PMA-modified waterborne acrylic resin was designed and synthesized. What is more, the methods of Fourier transform infrared spectroscopy (FT-IR), X-ray photoelectron spectroscopy (XPS), and scanning electron microscope (SEM) were used to analyze the structure of synthetic resin. This resin can be used as the main film-forming material of coating and exert its function in coating protection and other related fields.

Experimental

Materials

Methyl methacrylate (MMA, analytical grade), acrylic acid (AA, analytical grade), styrene (ST, analytical

grade), hydroxyethyl methacrylate (HEMA, analytical grade), glycidyl methacrylate (GMA, analytical grade), and N, N-dimethyl ethanolamine (DMEA, analytical grade) were supplied by Chengdu Cologne Chemical Co. 2-Butoxy ethanol (BCS, analytical reagent), vinyl tertiary carbonate (veova-9, 99%), ethylene glycol (EG, analytical reagent), and benzoyl peroxide (BPO, chemical pure) were obtained from Tianjin Bodi Chemical Co. 1H,1H,5H-octafluoroamyl methacrylate (OF-PMA, analytical reagent) was provided by Fuxin Ruifeng Fluorine Chemical Co., Ltd. All the reagents were used as received without any further treatment.

Synthesis of waterborne acrylic resin modified by OF-PMA

Waterborne acrylic resin was prepared by a semi-continuous solution polymerization method. The reaction was carried out in a four-port flask with a mechanical stirring device, temperature gauge, and reflux condenser. The formulations for the unmodified resins are shown in Table 1. When the modified resin was synthesized, the type and amount of the reagents shown in Table 1 remained unchanged, only the amount of OF-PMA monomer changed. The synthesis process is as follows. First, ethylene glycol butyl ether was added to the four-port flask as the base solvent, and 0.2 g BPO was added when the experimental temperature rose to 91 °C. In order to investigate the influence of the addition methods of OF-PMA on the resin properties, the addition methods of monomers were divided into two types. The first type (a) was to mix all reagents evenly and drop them into a four-mouth flask within 2 h, as shown in Fig. 2a (named as “one-step dropping”). The second type (b) was to mix 0.5 g GMA, 1.5 g V9, 2.25 g HEMA, 3.0 g AA, 3.0 g St, 5.0 g EG, 5.0 g BCS and 12.0 g MMA, and then dropped them into a four-mouth flask through a constant pressure dropping funnel within 1.5 h. After holding for 0.5 h, the remaining HEMA, GMA and BCS and OF-PMA monomer were mixed and dropped into the four-mouth flask within 30 min, as shown in Fig. 2b (named as “two-step dropping”). After adding the monomers, the reaction was kept at 91 °C for 2 h, and 0.05 g BPO was added at the middle of two hours. The four-mouth flask was cooled down to room temperature after reaction, and then, the products were filtered with a filter cloth. Finally, an

appropriate amount of DMEA was added to adjust pH to 8, and the final products were obtained.

Preparation of coating film

The preparation of coating film was divided into four steps. Firstly, 4.5 cm × 9 cm tinplate substrate was polished with sandpaper, wiped with alcohol, and then put aside for use. Secondly, 5 g as-prepared resin was adjusted to pH 8 with DMEA, and then, 5 g deionized water was added. The mixture was stirred evenly and put it aside for use. The third step, the waterborne acrylic resin prepared in the second step was uniformly coated on the tinplate prepared in the first step with 60- μ m steel wires. Finally, the resin-coated iron plate was cured in the oven at 140 °C for 20 min and then removed for performance test.

Table 1 Formulations for unmodified resins

Component	Chemical	Mass (g)
Monomer	V9	1.5
	GMA	1.5
	St	3.0
	AA	3.0
	HEMA	3.75
	MMA	12.0
Solvent	BCS	35.0
Solubilizer	EG	5.0
Initiator	BPO	0.35

Characterizations

About 2.0 g resin was taken and put it into a clean glass-surface vessel. The oven temperature was set to 150 °C to remove the volatile matter until the mass difference between the two weights after an interval of 2 h was less than 0.01 g. The solid content G can be calculated by formula (1):

$$G = \frac{M_2 - M_0}{M_1 - M_0} \times 100\% \quad (1)$$

where M_0 , M_1 , and M_2 refer to the mass of the glass-surface vessel, the total mass of the glass-surface vessel and resin, and the total mass of the glass-surface vessel and resin after drying, respectively. The monomer conversion C is calculated by Eq. (2):

$$C = \frac{M \times G - m}{w} \quad (2)$$

where M refers to the total feeding amount; m refers to the weight of non-volatile substances; and w refers to the weight of the monomer.

The basic physical properties of resin coating such as water resistance, adhesion, pencil hardness, and impact resistance were determined according to the standard Γ OCT 9.403:1980, ISO 2409:2013, ISO 15184:2012 and ISO 6272–2:2011, respectively. The details are stated in the Supplementary Data.

The determination methods of FT-IR, DSC, TGA, XPS, contact angle, and tensile property can all be found in Supplementary Data.

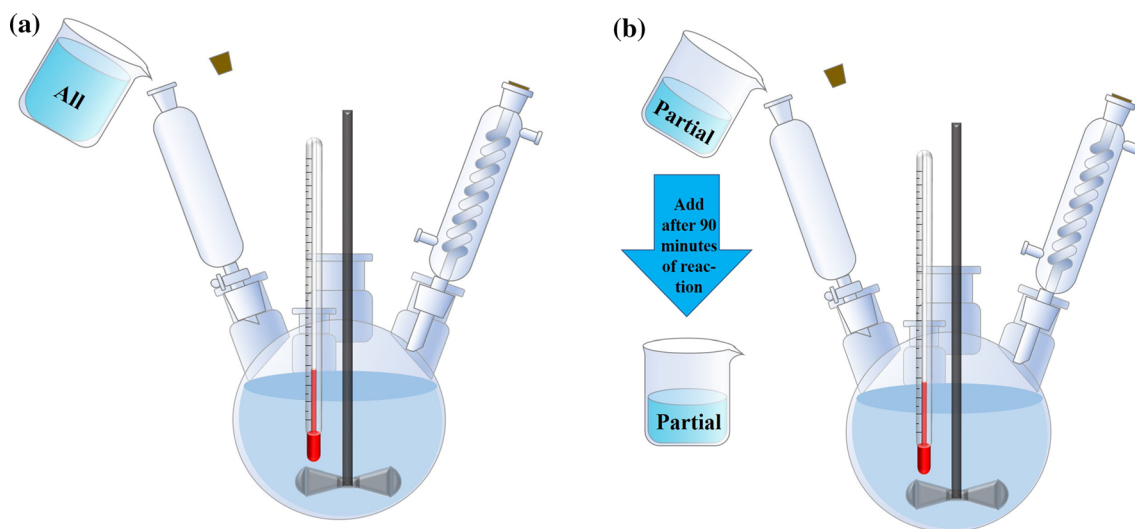


Figure 2 Schematic diagram of monomer adding method: **a** one-step dropping and **b** two-step dropping.

Results and discussion

The effect of the addition method of OF-PMA monomer on resin properties

The influences of different ways of adding monomers exerted heterogenous on the properties of the resin were studied. The influences of the fluorine monomer addition method on polymerization conversion and resin coating hardness are shown in Table 2.

The appearance of the resin synthesized by the two dropping methods shows no remarkable difference, both of which are colorless and transparent. It is shown in Table 2 that the conversion rate of one-step dropping method is more than 98%, which is higher than that of two-step dropping method (about 94.5%), and the hardness of the resin film prepared by one-step dropping method is much higher than that of two-step method. The possible reason is that the fluorine monomer and other monomers can be mixed evenly in the one-step dropping method, so that the monomers can react fully with each other, the conversion rate is higher, and the resin performance is better. In addition, all the film adhesions of the resins obtained by two methods are 0 grade, which are recorded as Gt0. Therefore, one-step dropping method was chosen as the addition method of OF-PMA monomer.

Characterization of chemical structure

The changes of functional groups in the resin before and after modification were analyzed by FT-IR as shown in Fig. 3. It can be seen that there are

pronounced absorption peaks of -OH and C-H at 3436 and 2957 cm^{-1} , respectively. The significant peaks at 1388 and 1457 cm^{-1} correspond to the characteristic absorbance of CH_2 and CH_3 groups. The sharp peaks observed at 1734 cm^{-1} can be ascribed to the strong tensile vibration of $\text{C}=\text{O}$ [21]. The peaks at 1149 and 1242 cm^{-1} are attributed to the asymmetric and symmetric tensile vibrations of $\text{C}-\text{O}-\text{C}$. However, compared with the unmodified resin, the spectrum of the modified resin possesses a wider peak between 1119 and 1242 cm^{-1} [22, 23], owing to the overlapped stretching vibration of $\text{C}-\text{F}$ and $\text{C}-\text{O}-\text{C}$ [23–25], indicating that OF-PMA monomer has been introduced into the copolymer molecular chain by solution polymerization.

In order to further analyze the chemical structure of the polymer, the samples WA-F0 and WA-F3 were characterized by XPS. The results are shown in Fig. 4.

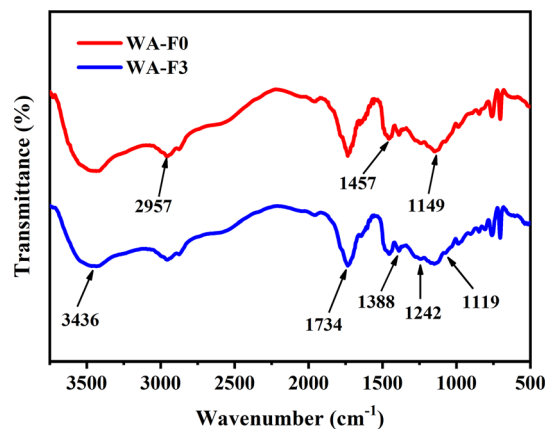


Figure 3 FT-IR spectra of waterborne acrylic resin.

Table 2 Effect of the fluorine monomer addition method on resin coating hardness and conversion rate

One-step dropping sample name	OF-PMA content (wt %) ^a	Coating hardness	Conversion rate (%)
WA-F0	0	3H	97.68
WA-F1	2.5	4H	98.05
WA-F2	5.0	4H	98.10
WA-F3	7.5	4H	98.54
WA-F4	10	4H	98.72
Two-step dropping sample name	OF-PMA content (wt %) ^a	Coating hardness	conversion rate (%)
WA-2-F0	0	2H	93.78
WA-2-F1	2.5	2H	94.52
WA-2-F2	5.0	2H	94.32
WA-2-F3	7.5	2H	94.68
WA-2-F4	10	2H	94.71

^aOF-PMA mass fraction in all monomers

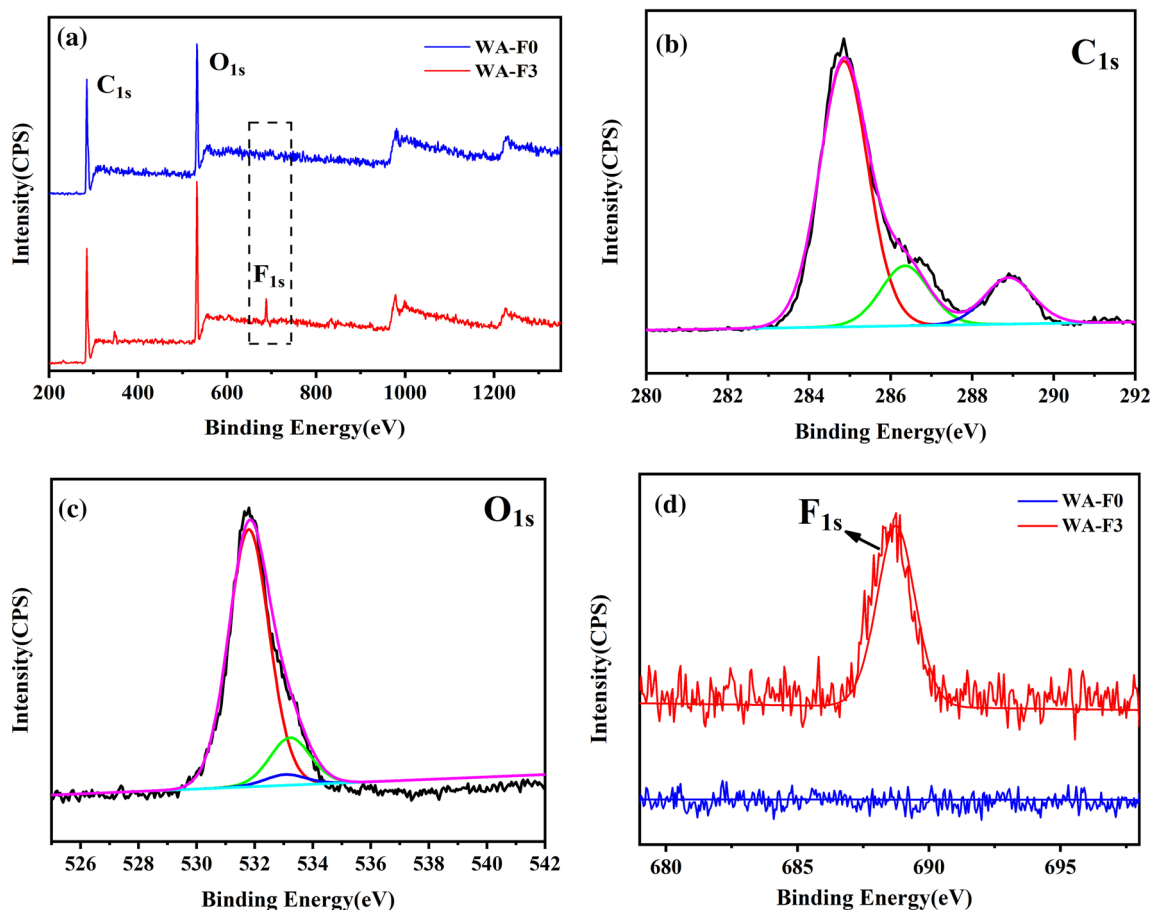


Figure 4 XPS spectra of waterborne acrylic resin films, **a** XPS full survey spectrum spectra, **b** spectra of C 1 s, **c** spectra of O 1 s, and **d** spectra of F 1 s.

In Fig. 4a, the strong characteristic signals of C1s orbit (286.23 eV) and O1s orbit (530.62 eV) can be observed in both samples [26]. The three main peaks of C1s (Fig. 4b) are at 288.88 eV, 286.38 eV, and 284.84 eV, respectively [27–29]. The peak at 288.88 eV belongs to the O=C=O, and the other two peaks correspond to the C=O and C–C bonds, respectively [15]. The track of O1s is shown in Fig. 4c. Compared with sample WA-F0, sample WA-F3 is equipped with the characteristic signal of an F1s orbit at 686.78 eV. In addition, a high-resolution spectrum of F1s is shown in Fig. 4d. The F1s characteristic peak of sample WA-F3 film is obvious, while that of sample WA-F0 resin film is close to a straight line without the F1s characteristic peak. Therefore, it can be concluded that fluorine has been enriched on the surface of WA-F3 resin film, and the monomer OF-PMA has been successfully introduced into the copolymer chain.

On the basis of the above discussion, the reaction mechanism was further explored. Figure 5 shows

some reactions that may occur during the resin polymerization and curing. Under the action of initiator (BPO), various monomers react with each other to form macromolecular chains. Resin curing is a process of dehydration and intermolecular condensation reaction to remove water molecules and form a complete coating [30]. In this process, low surface energy of fluorine atoms enables it easy to accumulate on the surface of resin coating, so as to achieve the effect of hydrophobicity [15]. In addition, the introduction of OF-PMA brings a lot of high-energy C-F to the molecular chain, changes the polymer structure, and achieves the effect of the mechanical strength and thermal properties of the resin.

Analysis of water resistance

To evaluate the water resistance of the resin coating, the contact angle and the water resistance time of the film were measured, respectively. The test results are

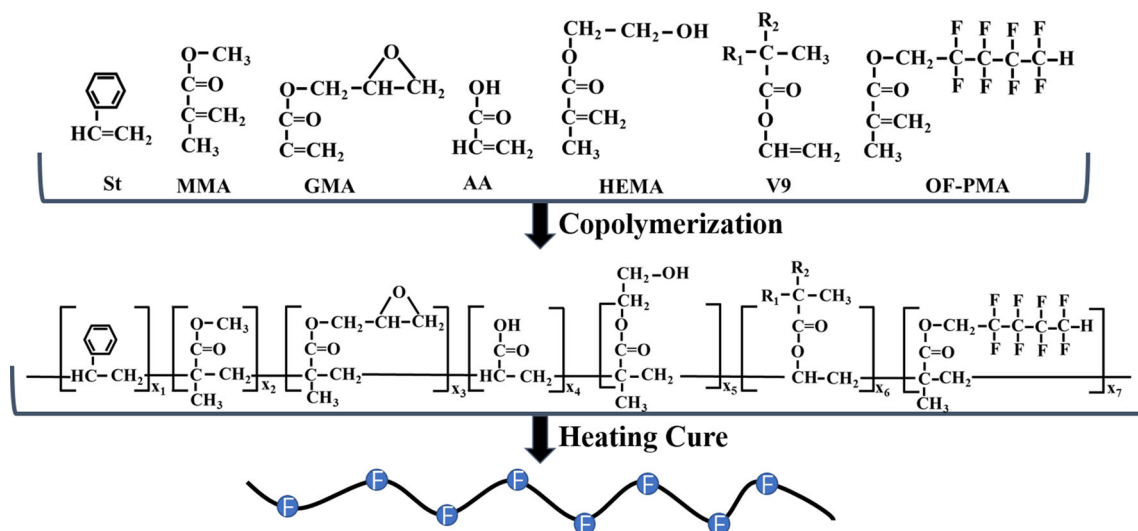


Figure 5 Possible reactions of polymers during polymerization and curing.

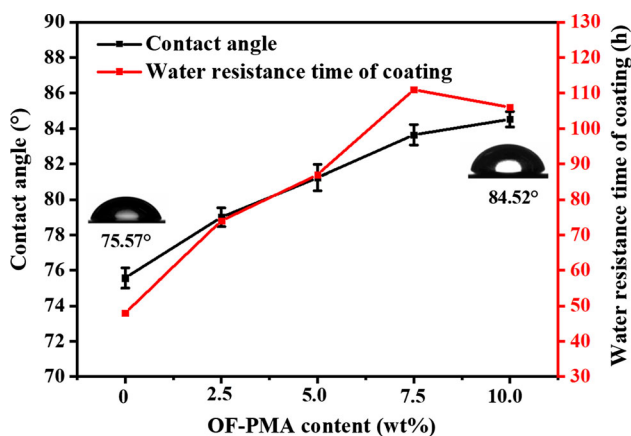


Figure 6 Effect of OF-PMA content on contact angle and water resistance time of resin coating.

shown in Fig. 6. It is evidenced that the contact angle and water resistance time of the resin coating increase with increasing the amount of OF-PMA monomer. The introduction of OF-PMA increased the contact angle of the resin coating from 75.57° to 84.52° and improved the water resistance time from 48 to 111 h. The possible reason is that there exist 8 low-surface energy fluorine atoms in each fluoroalkyl side chain of OF-PMA monomer. In the process of film forming, the fluoroalkyl chain segments will preferentially aggregate to the air surface [16, 22, 31], thus reducing the coating surface energy and enhancing water resistance.

In order to further explore the water resistance, we studied the surface energy (γ_s) of resin coating, which can be calculated by Neumann's equation [32, 33] as shown by Eq. (3):

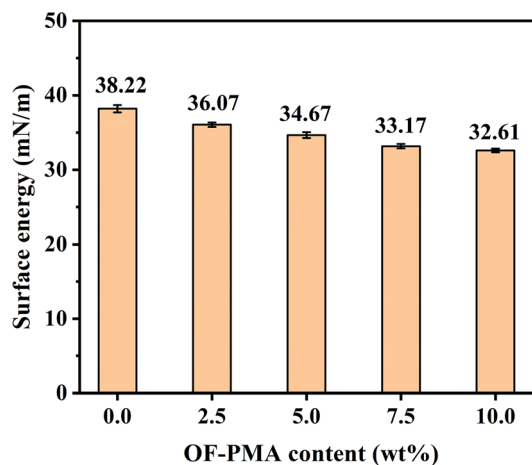


Figure 7 Impact of OF-PMA content on surface energy.

$$\cos \theta = 2 \sqrt{\frac{\gamma_s}{\gamma_L}} \cdot e^{-\beta(\gamma_L - \gamma_s)^2} - 1 \quad (3)$$

where θ is the contact angle of resin coating measured experimentally; β is a constant summarized by measuring the contact angle of different types of solids, and its mean value is $0.0001247 \text{ (m}^2 \cdot \text{mJ}^{-1})^2$ [34]; γ_L is the vapor surface energy of water at room temperature (about $72.75 \text{ (mN} \cdot \text{m}^{-1})$) [30, 32]. Calculated from Formula (3), the results of γ_s are shown in Fig. 7. It can be discovered that the γ_s of the resin coating is negatively correlated with the contact angle of the resin coating. With the contact angle increased from 75.57° to 84.52°, the γ_s of the coating decreased from 38.22 to 32.61 mN m^{-1} , resulting in the increment of

hydrophobicity and water resistance of waterborne acrylic resin [35].

However, when the content of OF-PMA monomer is more than 7.5%, the water resistance time begins to decrease. This may be because when too many OF-PMA monomers are introduced, the C–F bonds on the long fluorocarbon chain are also greatly increased, resulting in the decrease of the compatibility between OF-PMA monomers and some hydrophilic groups in the polymerization process due to the polarity difference among them [15, 26]. Based on the above analysis, it can be concluded that the water resistance of the modified resin is better when the content of OF-PMA is 7.5%.

Thermal performance analysis

The curing behavior of the modified waterborne acrylic resins with different OF-PMA contents was detected by DSC, as shown in Fig. 8. It can be seen that the DSC curve is very smooth with only one exothermic peak, demonstrating a uniform coating formed during the curing process. For unmodified resin, the curing temperature of the resin is only 82.29 °C. After introducing OF-PMA monomer, the endothermic peak of the curing reaction gradually shifted to higher temperature with increasing the content [26]. When the content of OF-PMA is 10%, the curing temperature of the resin reaches 106.46 °C, indicating that OF-PMA reacts with other monomers and the chain structure changes. Compared with the unmodified acrylic resin, the addition of OF-PMA changed the structure of the polymer macromolecular chain. The long fluorinated chain enhanced the entanglement between resin molecules, increased

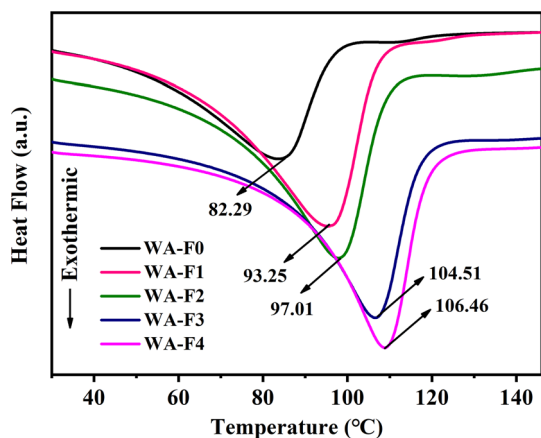


Figure 8 DSC curves of different OF-PMA monomer contents.

glass transition temperature (T_g), and enhanced the thermal stability of waterborne acrylic resin [36].

In addition, the thermal degradation behavior of waterborne acrylic resin was studied by thermogravimetric analyzer (TGA). The TGA curves of the resin films with different contents of OF-PMA monomer are shown in Fig. 9. All resin samples experienced two thermal decomposition processes. The first decomposition process is from 100 to 300 °C, in which the mass loss is not only the removal of water molecules, residual acrylic acid, acrylate monomers, and DEMA volatilization, but also the decomposition of some short-chain polymers [18, 37]. When the temperature rises to 300 °C, the macromolecular polymer begins to decompose, the residue rates of the samples are decreased to 67.02%, 73.33%, 78.43%, 79.76%, and 79.14%, respectively. During the secondary decomposition at 300–470 °C, the main weight loss of the sample is due to the decomposition of macromolecular chains in the polymer. The final residue rate of the sample is increased from 0.75% (WA-F0) to 2.71% (WA-F4). It can be found that with the increase of OF-PMA monomer content, the weight loss rate of the resin is gradually reduced, which further demonstrates the improved thermal stability of the resin through modification by fluorine monomer. The reason is that the introduction of OF-PMA monomer is equipped with large molecular weight and a large number of high-energy bonds C–F. After reacting with other monomers, the number and length of long-chain polymer molecules increase; therefore, destroying the internal chemical bond to decompose the polymer requires more energy [16, 22, 38].

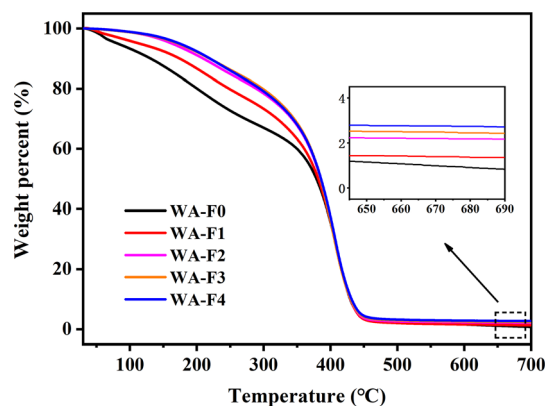


Figure 9 TGA curves of different OF-PMA monomer contents.

Analysis of the mechanical property

The stress–strain curve, tensile strength, elongation at break, and Young's modulus of resin with different OF-PMA monomer content were studied, and the results are shown in Fig. 10 and Table 3. It is indicated that the tensile strength, elongation at break, and Young's modulus of the resin are improved after the introduction of OF-PMA monomer. The tensile strength was increased by 92.7% (from 15.44 to 29.75 MPa), Young's modulus was increased by 65.5% (from 667 to 1104 MPa), and the elongation at break was increased by 5.57% (from 4.35 to 9.92%). The reason may be that the introduction of OF-PMA monomer with a relatively high T_g can make copolymer possess better rigidity [22], and make the sample more difficult to be broken [39]. When the content of OF-PMA is increased to 10%, the tensile strength of the sample begins to decrease. In addition, the addition of too many OF-PMA monomers can reduce the compatibility between monomers, resulting in a greatly reduced cohesion between molecules and the repulsion behavior in the resin [15, 40]. When the influence of repulsion behavior exceeds the increase of molecular chain strength, the external force is applied to the film and the stress transfer in the polymer becomes worse, and finally the tensile strength of the sample decreases. The increase of percentage of breaking elongation is also due to the repulsive behavior within the resin molecules. In addition, the final strain of all samples does not exceed 10%, and the stress–strain relationship is linear. The samples break after reaching the elastic limit, which belongs to the elastic deformation

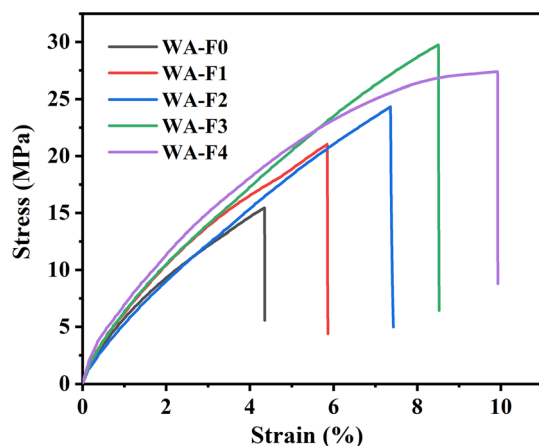


Figure 10 Stress–strain curves of resins with different OF-PMA contents.

[41, 42]. From the above analysis, when the content of OF-PMA monomer is 7.5%, the mechanical properties of the resin are the best.

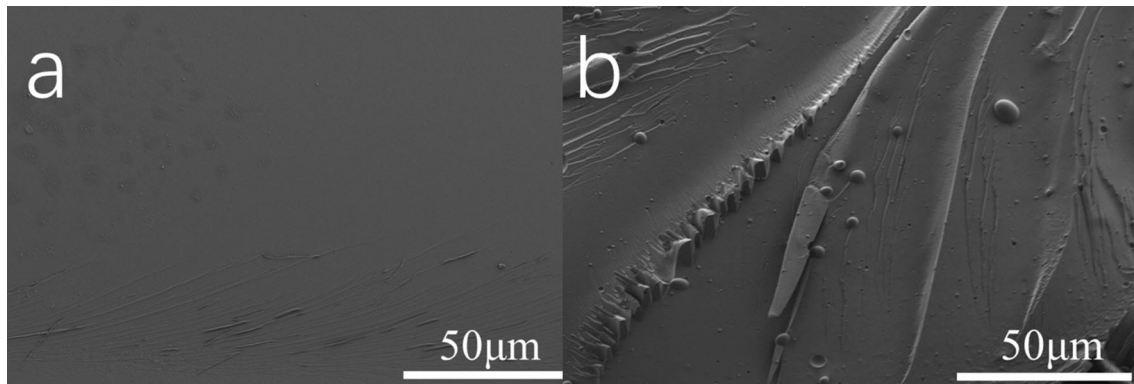
The improvement in the tensile strength of resin samples was further confirmed by SEM. The images are shown in Fig. 11. It is shown that the SEM images of the rupture surfaces of the resin tensile sample of the unmodified resin sample are relatively uniform and flat (Fig. 11a), while that of WA-F3 is fibrous and irregular (Fig. 11b), indicating that the rigidity of the resin increases after modification. The possible reason is that the introduced OF-PMA reacts with other monomers, which makes the molecular chain structure more complex, and the fluorine-containing blocks will migrate and enrich the surface during the curing stage, thus increasing the interaction between molecules in the resin [39].

Conclusions

A novel waterborne acrylic resin modified by OF-PMA was successfully synthesized by the solution polymerization method. After introducing OF-PMA with a large number of high-energy C–F bonds into acrylic resin, the polymer structure has been changed, the fluorine atoms with low surface energy in the polymer tend to migrate to the coating surface, which improves the water resistance, heat resistance and mechanical properties of the resin. What is more, when the content of OF-PMA monomer reached 7.5%, the tensile strength of the resin sample reached 29.75 MPa, and the water resistance time of the coating reached up to 111 h, which was much higher than that of the unmodified resin. However, the introduction of excessive OF-PMA monomers into the resin would increase the intermolecular polarity difference and decrease the polymer intermolecular cohesion, leading to repulsion behavior and reduced tensile strength and water resistance. Therefore, only when the concentration of OF-PMA was 7.5%, the comprehensive properties of the modified resin were the best. With high mechanical strength, good heat resistance, and water resistance, the waterborne resin can be used as the main film-forming material of coatings, which will also exhibit broad application prospects in coatings [43, 44], automotive coatings [45], and other fields like composites [46–51].

Table 3 The mechanical properties of the resin sample

Sample	Tensile strength (MPa)	Young's modulus (MPa)	Elongation at break (%)
WA-F0	15.44 ± 0.4	667 ± 43	4.35 ± 0.42
WA-F1	21.03 ± 0.3	758 ± 32	5.86 ± 0.35
WA-F2	24.33 ± 0.4	875 ± 34	7.42 ± 0.21
WA-F3	29.75 ± 0.6	1012 ± 22	8.52 ± 0.29
WA-F4	27.38 ± 0.5	1104 ± 56	9.92 ± 0.36

**Figure 11** SEM images of the rupture plane of the resin tensile sample: **a** WA-F0, and **b** WA-F3.

Acknowledgements

This work was supported by the Natural Science Foundation of Shandong Province (No. ZR2019BEE075), Scientific Research Foundation of SDUST for Recruited Talents (No. 2019RCJJ007), and Elite Program of SDUST (No. skr21-3-051). The authors acknowledge the financial support of Taif University Researchers Supporting Project number (TURSP-2020/14), Taif University, Taif, Saudi Arabia.

Declarations

Conflict of interest The authors declare that they do not have any commercial or associative interest that represents a conflict of interest in connection with the work submitted.

Supplementary Information: The online version contains supplementary material available at <http://doi.org/10.1007/s10853-022-07956-5>.

References

- [1] Zhu Q, Huang Y, Li Y et al (2021) Aluminum dihydric tripolyphosphate/polypyrrole-functionalized graphene oxide waterborne epoxy composite coatings for impermeability and corrosion protection performance of metals. *Adv Compos Hybrid Mater* 4:780–792. <https://doi.org/10.1007/s42114-021-00265-6>
- [2] Qiao G, Wang S, Wang X, Chen X, Wang X, Cui H (2022) Ni/Co/black phosphorus nanocomposites for Q235 carbon steel corrosion-resistant coating. *Adv Compos Hybrid Mater* 5:438–449. <https://doi.org/10.1007/s42114-021-00268-3>
- [3] Ashok RB, Srinivasa CV, Basavaraju B (2020) Study on morphology and mechanical behavior of areca leaf sheath reinforced epoxy composites. *Adv Compos Hybrid Mater* 3:365–374. <https://doi.org/10.1007/s42114-020-00169-x>
- [4] Song H, Zhang Q, Zhang Y et al (2021) Waterborne polyurethane/3-amino-polyhedral oligomeric silsesquioxane (NH₂-POSS) nanocomposites with enhanced properties. *Adv Compos Hybrid Mater* 4:629–638. <https://doi.org/10.1007/s42114-021-00285-2>
- [5] Yu Z, Yan Z, Zhang F et al (2022) Waterborne acrylic resin co-modified by itaconic acid and γ -methacryloxypropyl triisopropoxidesilane for improved mechanical properties, thermal stability, and corrosion resistance. *Prog Org Coat* 168:106875. <https://doi.org/10.1016/j.porgcoat.2022.106875>
- [6] Cai J, Murugadoss V, Jiang J et al (2022) Waterborne polyurethane and its nanocomposites: a mini-review for anti-corrosion coating, flame retardancy, and biomedical applications. *Adv Compos Hybrid Mater* 5:641–650. <https://doi.org/10.1007/s42114-022-00473-8>
- [7] Gao Q, Pan Y, Zheng G, Liu C, Shen C, Liu X (2021) Flexible multilayered MXene/thermoplastic polyurethane films with excellent electromagnetic interference shielding,

- thermal conductivity, and management performances. *Adv Compos Hybrid Mater* 4:274–285. <https://doi.org/10.1007/s42114-021-00221-4>
- [8] Llevot A, Meier M (2018) Perspective: green polyurethane synthesis for coating applications. *Polym Int* 68:826–831. <https://doi.org/10.1002/pi.5655>
- [9] Bustero I, Gaztelumendi I, Obieta I et al (2020) Free-standing graphene films embedded in epoxy resin with enhanced thermal properties. *Adv Compos Hybrid Mater* 3:31–40. <https://doi.org/10.1007/s42114-020-00136-6>
- [10] Liu C, Yin Q, Li X et al (2021) A waterborne polyurethane-based leather finishing agent with excellent room temperature self-healing properties and wear-resistance. *Adv Compos Hybrid Mater* 4:138–149. <https://doi.org/10.1007/s42114-021-00206-3>
- [11] Shao W, Liu D, Cao T et al (2021) Study on favorable comprehensive properties of superhydrophobic coating fabricated by polytetrafluoroethylene doped with graphene. *Adv Compos Hybrid Mater* 4:521–533. <https://doi.org/10.1007/s42114-021-00243-y>
- [12] Duan Y, Huo Y, Duan L (2017) Preparation of acrylic resins modified with epoxy resins and their behaviors as binders of waterborne printing ink on plastic film. *Colloids Surf A Physicochem Eng Aspects* 535:225–231. <https://doi.org/10.1016/j.colsurfa.2017.09.041>
- [13] Jiao C, Sun L, Shao Q et al (2021) Advances in waterborne acrylic resins: synthesis principle, modification strategies, and their applications. *ACS Omega* 6:2443–2449. <https://doi.org/10.1021/acsomega.0c05593>
- [14] Yang K, Chen X, Zhang Z, Yu X, Naito K, Zhang Q (2019) Introducing rigid pyrimidine ring to improve the mechanical properties and thermal-oxidative stabilities of phthalonitrile resin. *Polym Advan Technol* 31:328–337. <https://doi.org/10.1002/pat.4773>
- [15] Bai S, Zheng W, Yang G et al (2017) Synthesis of core-shell fluorinated acrylate copolymers and its application as finishing agent for textile. *Fibers Polym* 18:1848–1857. <https://doi.org/10.1007/s12221-017-7228-2>
- [16] Lei H, He D, Guo Y, Tang Y, Huang H (2018) Synthesis and characterization of UV-absorbing fluorine-silicone acrylic resin polymer. *Appl Surf Sci* 442:71–77. <https://doi.org/10.1016/j.apsusc.2018.02.134>
- [17] Çakmakçı E (2018) HDI trimer based fluorine containing urethane methacrylates for hydrophobic photocured coatings. *Polym-Plast Tech Mat* 58:854–865. <https://doi.org/10.1080/03602559.2018.1520260>
- [18] Jiao C, Shao Q, Wu M et al (2020) 2-(3,4-Epoxy) ethyltriethoxysilane-modified waterborne acrylic resin: preparation and property analysis. *Polymer* 190:122196. <https://doi.org/10.1016/j.polymer.2020.122196>
- [19] Liu Z, Fan X, Zhang J et al (2021) Improving the comprehensive properties of PBO fibres/cyanate ester composites using a hyperbranched fluorine and epoxy containing PBO precursor. *Compos Part A Appl S* 150:106596. <https://doi.org/10.1016/j.compositesa.2021.106596>
- [20] Tan X, Wang Y, Huang Z et al (2021) Facile fabrication of a mechanical, chemical, thermal, and long-term outdoor durable fluorine-free superhydrophobic coating. *Adv Mater Interfaces* 8:2002209. <https://doi.org/10.1002/admi.202002209>
- [21] Hao G, Zhu L, Yang W, Chen Y (2015) Investigation on the film surface and bulk properties of fluorine and silicon contained polyacrylate. *Prog Org Coat* 85:8–14. <https://doi.org/10.1016/j.porgcoat.2015.02.021>
- [22] Fang C, Zhu K, Zhu X, Lin Z (2019) Preparation and characterization of self-crosslinking fluorinated polyacrylate latexes and their pressure sensitive adhesive applications. *Int J Adhes Adhes* 95:102417. <https://doi.org/10.1016/j.ijadh.2019.102417>
- [23] Wang Y, Qiu F, Xu B et al (2013) Preparation, mechanical properties and surface morphologies of waterborne fluorinated polyurethane-acrylate. *Prog Org Coat* 76:876–883. <https://doi.org/10.1016/j.porgcoat.2013.02.003>
- [24] Lee SW, Lee YH, Park H, Kim HD (2013) Effect of total acrylic/fluorinated acrylic monomer contents on the properties of waterborne polyurethane/acrylic hybrid emulsions. *Macromol Res* 21:709–718. <https://doi.org/10.1007/s13233-013-1122-6>
- [25] Wang Y, Long J, Bai Y et al (2015) Preparation and characterization of fluorinated acrylic pressure sensitive adhesives for low surface energy substrates. *J Fluorine Chem* 180:103–109. <https://doi.org/10.1016/j.jfluchem.2015.09.007>
- [26] Lü T, Qi D, Zhang D, Liu Q, Zhao H (2016) Fabrication of self-cross-linking fluorinated polyacrylate latex particles with core-shell structure and film properties. *React Funct Polym* 104:9–14. <https://doi.org/10.1016/j.reactfunctpolym.2016.04.020>
- [27] Yin X, Sun C, Zhang B et al (2017) A facile approach to fabricate superhydrophobic coatings on porous surfaces using cross-linkable fluorinated emulsions. *Chem Eng J* 330:202–212. <https://doi.org/10.1016/j.cej.2017.06.145>
- [28] Cheng W, Wang Y, Ge S, Ding X, Cui Z, Shao Q (2021) One-step microwave hydrothermal preparation of Cd/Zr-bimetallic metal-organic frameworks for enhanced photochemical properties. *Adv Compos Hybrid Mater* 4:150–161. <https://doi.org/10.1007/s42114-020-00199-5>
- [29] Zheng J, Sun L, Jiao C et al (2021) Hydrothermally synthesized Ti/Zr bimetallic MOFs derived N self-doped TiO₂/ZrO₂ composite catalysts with enhanced photocatalytic

- degradation of methylene blue. *Colloid Surf A* 623:126629. <https://doi.org/10.1016/j.colsurfa.2021.126629>
- [30] Zheng B, Ge S, Wang S et al (2020) Effect of γ -aminopropyltriethoxysilane on the properties of cellulose acetate butyrate modified acrylic waterborne coatings. *React Funct Polym* 154:104657. <https://doi.org/10.1016/j.reactfunctpolym.2020.104657>
- [31] Li H, Zhou J, Zhao J, Li Y, Lu K (2020) Synthesis of cellulose nanocrystals-armed fluorinated polyacrylate latexes via pickering emulsion polymerization and their film properties. *Colloids Surf B Biointerfaces* 192:111071. <https://doi.org/10.1016/j.colsurfb.2020.111071>
- [32] Liu J, Huang J, Wujcik EK et al (2015) Hydrophobic electrospun polyimide nanofibers for self-cleaning materials. *Macromol Mater Eng* 300:358–368. <https://doi.org/10.1002/mame.201400307>
- [33] Wu M, Ge S, Jiao C et al (2020) Improving electrical, mechanical, thermal and hydrophobic properties of waterborne acrylic resin-glycidyl methacrylate (GMA) by adding multi-walled carbon nanotubes. *Polymer* 200:122547. <https://doi.org/10.1016/j.polymer.2020.122547>
- [34] Li J, Zhang H, Liu F, Lai J, Qi H, You X (2013) A new series of fluorinated alicyclic-functionalized polyimides derived from natural-(D)-camphor: synthesis, structure-properties relationships and dynamic dielectric analyses. *Polymer* 54:5673–5683. <https://doi.org/10.1016/j.polymer.2013.08.014>
- [35] Yu F, Gao J, Liu C et al (2020) Preparation and UV aging of nano-SiO₂/fluorinated polyacrylate polyurethane hydrophobic composite coating. *Prog Org Coat* 141:105556. <https://doi.org/10.1016/j.porgcoat.2020.105556>
- [36] He S, Liu W, Yang M, Liu C, Jiang C, Wang Z (2018) Fluorinated polyacrylates containing amino side chains for the surface modification of waterborne epoxy resin. *J Appl Polym Sci* 136:47091. <https://doi.org/10.1002/app.47091>
- [37] Guo X, Ge S, Wang J et al (2018) Waterborne acrylic resin modified with Glycidyl Methacrylate (GMA): formula optimization and property analysis. *Polymer* 143:155–163. <https://doi.org/10.1016/j.polymer.2018.04.020>
- [38] Lei H, He D, Guo Y, Tang Y, Lu Y (2018) Modification of a fluorine-silicone acrylic resin with a free-radical-catching agent. *J Appl Polym Sci* 135:46385. <https://doi.org/10.1002/app.46385>
- [39] Drake I, Cardoen G, Hughes A et al (2019) Polyurea-acrylic hybrid emulsions: characterization and film properties. *Polymer* 181:121761. <https://doi.org/10.1016/j.polymer.2019.121761>
- [40] Pang AL, Ismail H, Bakar AA (2016) Tensile properties, water resistance, and thermal properties of linear low-density polyethylene/polyvinyl alcohol/kenaf composites: effect of 3-(trimethoxysilyl) propyl Methacrylate (TMS) as a silane coupling agent. *BioResources* 11:5889
- [41] Öttinger MLHC, Suter UW (1991) Bond-length and bond-angle distributions in coarse-grained polymer chains. *J Chem Phys* 95:2178–2182. <https://doi.org/10.1063/1.460965>
- [42] Flory PJ, Hoeve CAJ, Ciferri A (1959) Influence of bond angle restrictions on polymer elasticity. *J Polym Sci* 34:337–347
- [43] Madhusudhana AM, Mohana KNS, Hegde MB, Nayak SR, Rajitha K, Swamy NK (2020) Functionalized graphene oxide-epoxy phenolic novolac nanocomposite: an efficient anticorrosion coating on mild steel in saline medium. *Adv Compos Hybrid Mater* 3:141–155. <https://doi.org/10.1007/s42114-020-00142-8>
- [44] Fan X, Liu Z, Huang J et al (2022) Synthesis, curing mechanism, thermal stability, and surface properties of fluorinated polybenzoxazines for coating applications. *Adv Compos Hybrid Mater* 5:322–334. <https://doi.org/10.1007/s42114-021-00381-3>
- [45] Naik V, Kumar M, Vijayan V, Kaup a, (2022) A review on natural fiber composite material in automotive applications. *Eng Sci* 18:1–10. <https://doi.org/10.30919/es8d589>
- [46] Dai B, Ma Y, Dong F et al (2022) Overview of MXene and conducting polymer matrix composites for electromagnetic wave absorption. *Adv Compos Hybrid Mater* 5:704–754. <https://doi.org/10.1007/s42114-022-00510-6>
- [47] Yao F, Xie W, Ma C et al (2022) Superb electromagnetic shielding polymer nanocomposites filled with 3-dimensional p-phenylenediamine/aniline copolymer nanofibers@copper foam hybrid nanofillers. *Compos Part B Eng* 245:110236. <https://doi.org/10.1016/j.compositesb.2022.110236>
- [48] Cao Y, Weng M, Mahmoud MHH et al (2022) Flame-retardant and leakage-proof phase change composites based on MXene/polyimide aerogels toward solar thermal energy harvesting. *Adv Compos Hybrid Mater* 5:1253–1267. <https://doi.org/10.1007/s42114-022-00504-4>
- [49] Wang P, Song T, Abo-Dief HM et al (2022) Effect of carbon nanotubes on the interface evolution and dielectric properties of polylactic acid/ethylene-vinyl acetate copolymer nanocomposites. *Adv Compos Hybrid Mater*. <https://doi.org/10.1007/s42114-022-00489-0>
- [50] Jing X, Li Y, Zhu J et al (2022) Improving thermal conductivity of polyethylene/polypropylene by styrene-ethylene-propylene-styrene wrapping hexagonal boron nitride at the phase interface. *Adv Compos Hybrid Mater*. <https://doi.org/10.1007/s42114-42022-00438-x>. <https://doi.org/10.1007/s42114-022-00438-x>
- [51] Kong D, El-Bahy ZM, Algadi H et al (2022) Highly sensitive strain sensors with wide operation range from strong MXene-composited polyvinyl alcohol/sodium

carboxymethylcellulose double network hydrogel. *Adv Compos Hybrid Mater.* <https://doi.org/10.1007/s42114-022-00531-1>

Publisher's Note Springer Nature remains neutral with regard to jurisdictional claims in published maps and institutional affiliations.

Springer Nature or its licensor (e.g. a society or other partner) holds exclusive rights to this article under a publishing agreement with the author(s) or other rightsholder(s); author self-archiving of the accepted manuscript version of this article is solely governed by the terms of such publishing agreement and applicable law.